JOURNAL OF MOLECULAR SPECTROSCOPY **190,** 107–111 (1998)
ARTICLE NO. MS987561

Tunable Far-Infrared Spectroscopy of $^{82}KrD^+$, $^{84}KrD^+$, $^{86}KrD^+$, and $^{82}KrH^+$

Hitoshi Odashima,* Fusakazu Matsushima,* Atsushi Kozato,* Shozo Tsunekawa,* Kojiro Takagi,* and Harold Linnartz†

*Department of Physics, Toyama University, Gofuku 3190, Toyama 930-8555, Japan; and †Institute for Physical Chemistry, University of Basel, Klingelbergstrasse 80, CH-4056 Basel, Switzerland

Received December 17, 1997; in revised form February 17, 1998

Pure rotational spectra of isotopic species of protonated krypton $^{82}KrD^+$, $^{84}KrD^+$, $^{86}KrD^+$, and $^{82}KrH^+$ were observed in the 0.75–3.5 THz region, using a tunable far-infrared radiation source. Rotational parameters B, D, and H of these molecular ions were determined. By analyzing the observed frequencies with the previous data on all the isotopic species, the mass independent Dunham parameters U_{kl}, Δ_{kl}^{Kr}, and Δ_{kl}^{H} have been improved.

1. INTRODUCTION

Protonated rare gas ions, such as HeH^+ (*1, 2, 3*), NeH^+ (*4, 5*), ArH^+, KrH^+ (*6*), and XeH^+ (*7*), have been studied extensively in the infrared (IR) region; their rotation–vibration transitions and high-J pure rotational transitions of ArH^+ ($J > 20$) (*8*) and HeH^+ ($J > 10$) (*3*) were observed. Few studies have been performed in the far-infrared (FIR) region in which most of their pure rotational transitions lie, because it is difficult to generate coherent, tunable FIR radiation for high-resolution spectroscopy. In the lower end of the FIR (less than 0.6 THz), only low-J pure rotational transitions of the heavier ions were observed (*9–14*). For higher frequencies, the tunable far-infrared (TuFIR) spectrometer developed by Evenson *et al.* has extended measurements into the terahertz region (*15, 16*). This technique has been successfully applied to the observation of pure rotational transitions of HeH^+ (*17*), NeH^+ (*18*), ArH^+ (*19*), and KrH^+ (*20*) up to 5 THz with an accuracy better than a few hundred kilohertz. For HeH^+ (*17*) and NeH^+ (*18*), systematic measurements of the isotopic species were made, and the molecular parameters were improved considerably by combining the accurate FIR data with the previous IR data.

The protonated krypton ion has 12 stable isotopic species which consist of a combination of six krypton isotopes (^{78}Kr, ^{80}Kr, ^{82}Kr, ^{83}Kr, ^{84}Kr, and ^{86}Kr) and two hydrogen isotopes (^1H and ^2D). Johns observed rotation–vibration transitions of all the KrH^+ isotopic species except for $^{78}KrH^+$ with a Fourier transform spectrometer in the IR region and determined the mass independent Dunham parameters (*6*). Warner *et al.* observed the $J = 1 \leftarrow 0$ transitions of KrD^+ for all the six krypton isotopes with a millimeter-wave spectrometer and determined the Born–Oppenheimer breakdown parameters Δ_{01}^{Kr} and Δ_{01}^{H} (*12*). They resolved hyperfine structures of $^{83}KrD^+$ due to the nuclear spin ($I = 9/2$) of ^{83}Kr and determined both its quadrupole coupling constant eqQ and its nuclear coupling constant C_N. Linnartz *et al.* observed the Zeeman splitting of the $J = 1 \leftarrow 0$ $^{84}KrH^+$ transition and those of the $J = 2 \leftarrow 1$ transitions of $^{84}KrD^+$ and $^{86}KrD^+$ (*13*) in a magnetic field-enhanced anomalous discharge (*21*), and determined experimentally the electric dipole moment of these ions. Recently, Linnartz *et al.* observed the pure rotational transitions of $^{84}KrH^+$ and $^{86}KrH^+$ up to $J = 7 \leftarrow 6$ with a TuFIR spectrometer (*20*). They determined the rotational parameters B, D, and H for these ions and improved the mass-independent Dunham parameters U_{01} and Δ_{01}^{H}. Rotational transitions of the 10 isotopic species other than these two ions have been left to be studied in the FIR region. With their accurate FIR frequencies, the mass-independent Dunham parameters of the protonated krypton ion will be improved.

In this paper we report the observation of the pure rotational transitions of $^{82}KrD^+$, $^{84}KrD^+$, $^{86}KrD^+$, and $^{82}KrH^+$ in the ground vibrational state with a TuFIR spectrometer. Rotational parameters B, D, and H of these ions were determined from our data and low-J transition frequencies reported in Refs. (*12*) and (*13*). These observed frequencies were also analyzed by combining with the previous data on both pure rotational transitions (*12, 13, 20*) and rotation–vibration transitions (*6*) of all the isotopic species of the protonated krypton ion. The mass-independent Dunham parameters were improved, and the higher-order Born–Oppenheimer breakdown parameter Δ_{02}^{H} was determined.

2. EXPERIMENTAL DETAILS AND RESULTS

A TuFIR spectrometer was used to perform the experiment. Coherent, tunable FIR radiation with a frequency uncertainty less than 35 kHz is generated by mixing the radia-

0022-2852/98 $25.00

tion from two CO_2 lasers and a microwave sweeper in a W-Co metal-insulator-metal (MIM) diode. Tunability of the FIR radiation is obtained by tuning the microwave frequency. The atmospheric water vapor in the path of the FIR radiation outside the sample cell was purged with nitrogen gas to prevent its absorption of the FIR radiation. The FIR radiation after passing through the sample cell was detected with a silicon composite bolometer cooled to the lambda point of ^{4}He. Details of our TuFIR spectrometer were described in Ref. (*22*).

Protonated krypton gases (KrH^+ or KrD^+) were produced by a discharge in a mixture of krypton and hydrogen (H_2 or D_2) gases in a liquid-nitrogen-cooled Pyrex glass tube of 1.4 m in length and 16 mm in diameter with a pair of electrodes. The krypton gas has natural abundances of 0.35% ^{78}Kr, 2.25% ^{80}Kr, 11.6% ^{82}Kr, 11.5% ^{83}Kr, 57.0% ^{84}Kr, and 17.3% ^{86}Kr. Consequently, the 82, 83, 84, and 86 isotopic species can be observed without isotopically enriched gases. The pressure ratio of krypton to hydrogen was 10:1 at a total pressure of 35 Pa. We mainly used a 10-kHz-rate ac discharge. Details of this system were described before in Ref. (*17*). A discharge current of 700 mA p-p and a high voltage of 3 kV p-p were used typically. We also used a dc discharge in some of the measurements, because the ac discharge easily destroyed the MIM diode contact. A discharge current of 300 mA and a high voltage of 3 kV were used typically. The mean frequencies were determined by averaging two frequencies measured under the opposite-polarity high voltages to eliminate the systematic frequency shift (*12*). In our previous experiment, ion velocity modulation was used to detect light ions such as HeH^+ (*17*) and NeH^+ (*18*). For heavier ions such as KrH^+, however, it was found that this technique was not effective. Therefore, source modulation at 1 kHz was used to detect absorption signals with a lock-in amplifier. The line-center frequency was determined using a line-fitting program in which a baseline is taken into account (*23*).

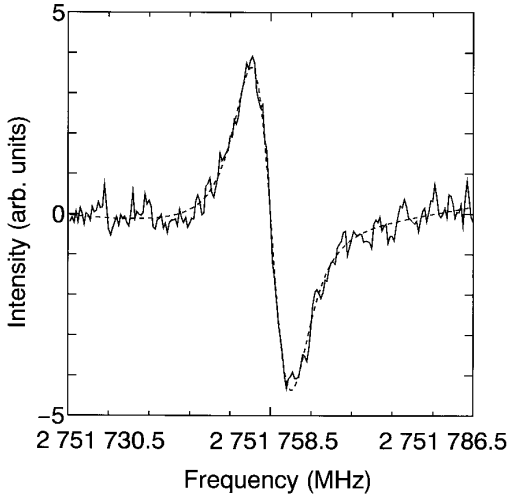

FIG. 1. Observed spectral line of the $J = 11 \leftarrow 10$ transition of $^{84}KrD^+$. The measured spectrum is the solid curve, and the fitted spectrum is the dashed curve.

TABLE 1
Observed Frequencies of Pure Rotational Transitions of $^{82}KrD^+$ (MHz)

$J' \leftarrow J''$	Observed frequency[a]	Obs. −Calc.[b]	Obs. −Calc.[c]
1 ← 0	251 688.279 (15)[d]	−0.035	−0.101
4 ← 3	1 006 058.570 (157)	−0.140	−0.298
5 ← 4	1 257 052.670 (56)[e]	0.016	−0.115
6 ← 5	1 507 699.731 (84)[e]	0.072	−0.003
7 ← 6	1 757 930.697 (72)[e]	0.141	0.146
8 ← 7	2 007 676.402 (59)[e]	0.112	0.205
9 ← 8	2 256 867.843 (229)	−0.107	0.070
10 ← 9	2 505 436.696 (53)[e]	−0.081	0.149
11 ← 10	2 753 314.062 (61)	−0.132	0.099
12 ← 11	3 000 432.001 (79)	0.181	0.337
13 ← 12	3 246 721.487 (132)	−0.003	−0.019

[a] The numbers in parentheses are the estimated 1σ uncertainties in units of the last quoted digits.
[b] Calculated frequency from the rotational parameters in Table 5.
[c] Calculated frequency from the mass independent Dunham parameters in Table 6.
[d] Ref. (*12*).
[e] Measured with a dc discharge.

We have observed the pure rotational spectra of $^{82}KrD^+$, $^{84}KrD^+$, $^{86}KrD^+$, and $^{82}KrH^+$. A plot of the observed absorption from the $J = 11 \leftarrow 10$ $^{84}KrD^+$ transition is shown in Fig. 1. The frequencies are listed in Tables 1–4 together with the observed − calculated (obs. − calc.) values calculated from the rotational parameters in Table 5 or from the mass independent Dunham parameters in Table 6. The $J = 1 \leftarrow 0$ transitions of all the four isotopic species mentioned above, the $J = 2 \leftarrow 1$ transitions of the three KrD^+ species, and the $J = 3 \leftarrow 2$ transition of $^{82}KrD^+$ were not observed because of poor signal-to-noise ratios. However, the averaged frequencies of two Zeeman components of the $J = 2 \leftarrow 1$ transitions of both $^{84}KrD^+$ and $^{86}KrD^+$ reported in Ref. (*13*) and the $J = 1 \leftarrow 0$ KrD^+ transition frequencies reported in Ref. (*12*) are included in Tables 1–3. The difference between the averaged frequencies and the zero-field frequencies of the $J = 2 \leftarrow 1$ transition of $^{84}KrD^+$ and $^{86}KrD^+$ at 503 GHz is estimated to be less than 100 kHz, because the average of the two Zeeman components of the $J = 1 \leftarrow 0$ $^{84}KrH^+$ transition at 494 GHz (*13*) is in agreement with the zero-field frequency within its 100 kHz uncertainty (*20*).

3. ANALYSIS AND DISCUSSION

The observed frequencies given in Tables 1–4 were fitted to the following effective Hamiltonian:

TABLE 2
Observed Frequencies of Pure Rotational Transitions of $^{84}KrD^+$ (MHz)

$J' \leftarrow J''$	Observed frequency[a]	Obs. −Calc.[b]	Obs. −Calc.[c]
1 ← 0	251 545.317 (10)[d]	−0.007	−0.068
2 ← 1	503 021.290 (25)[e]	0.029	−0.082
3 ← 2	754 358.353 (67)	−0.089	−0.230
4 ← 3	1 005 487.441 (39)	−0.097	−0.241
5 ← 4	1 256 339.145 (65)[f]	−0.136	−0.253
6 ← 5	1 506 844.538 (38)[f]	0.058	−0.002
7 ← 6	1 756 934.077 (41)[f]	0.035	0.052
8 ← 7	2 006 539.097 (37)[f]	0.104	0.206
9 ← 8	2 255 590.423 (83)	−0.075	0.103
10 ← 9	2 504 019.838 (40)[f]	−0.038	0.183
11 ←10	2 751 758.535 (54)	−0.093	0.116
12 ←11	2 998 738.337 (140)	−0.111	0.005
13 ←12	3 244 891.305 (64)	0.057	−0.024
14 ←13	3 490 149.183 (50)	0.007	−0.388

[a] The numbers in parentheses are the estimated 1σ uncertainties in units of the last quoted digits.
[b] Calculated frequency from the rotational parameters in Table 5.
[c] Calculated frequency from the mass independent Dunham parameters in Table 6.
[d] Ref.(*12*).
[e] Averaged frequency of two Zeeman components reported in Ref.(*13*).
[f] Measured with a dc discharge.

TABLE 3
Observed Frequencies of Pure Rotational Transitions of $^{86}KrD^+$ (MHz)

$J' \leftarrow J''$	Observed frequency[a]	Obs. −Calc.[b]	Obs. −Calc.[c]
1 ← 0	251 408.885 (15)[d]	−0.022	−0.084
2 ← 1	502 748.709 (75)[e]	0.207	0.093
3 ← 2	753 949.343 (168)	−0.149	−0.294
4 ← 3	1 004 942.478 (97)	−0.148	−0.296
5 ← 4	1 255 658.634 (47)[f]	−0.075	−0.195
6 ← 5	1 506 028.813 (46)[f]	0.188	0.125
7 ← 6	1 755 983.358 (68)[f]	0.000	0.016
8 ← 7	2 005 454.036 (69)[f]	0.028	0.132
9 ← 8	2 254 371.671(46)	−0.143	0.040
10 ← 9	2 502 668.187 (69)[f]	0.015	0.247
11 ←10	2 750 274.754 (57)	0.102	0.325
12 ←11	2 997 122.925 (202)	−0.100	0.034
13 ←12	3 243 145.220 (185)	−0.056	−0.113
14 ←13	3 488 273.618 (67)	−0.008	−0.375

[a] The numbers in parentheses are the estimated 1σ uncertainties in units of the last quoted digits.
[b] Calculated frequency from the rotational parameters in Table 5.
[c] Calculated frequency from the mass independent Dunham parameters in Table 6.
[d] Ref.(*12*).
[e] Averaged frequency of two Zeeman components reported in Ref.(*13*).
[f] Measured with a dc discharge.

$$H_{\text{eff}} = BJ(J+1) - D[J(J+1)]^2 + H[J(J+1)]^3. \quad [1]$$

The rotational parameters B, D, and H determined for each species are given in Table 5. The obs. − calc. values do not decrease even when a higher-order term $L[J(J+1)]^4$ is included in Eq. [1]. The obs. − calc. values exceed the estimated experimental uncertainties of the observed frequencies by a few hundred kilohertz for several transitions. This can be explained by systematic frequency shifts due to distorted baselines which originate from standing waves between the MIM diode and the detector. No systematic error is found for the measurements performed with the dc discharge. The ratio of the observed difference between opposite-polarity frequencies to their averaged frequency was about $10^{-8} \sim 10^{-7}$, which gives an ion drift velocity similar to that for the $J = 1 \leftarrow 0$ KrD^+ transition (*12*). Since this value gives a frequency difference of 25 ∼ 250 kHz at 2.5 THz, a systematic error in the averaged frequency, which should be much less than this difference of 250 kHz, is negligibly smaller than the systematic error due to the distorted baseline.

The observed frequencies in Tables 1–4 were also analyzed with the previous data on all the isotopic species of the protonated krypton ion according to the Dunham's expression (*24*):

$$E_{vJ} = \sum_{kl} Y_{kl}(v + 1/2)^k[J(J+1)]^l, \quad [2]$$

where

$$Y_{kl} = \mu_c^{-(k/2+l)} U_{kl}[1 + (m_e/M_{\text{Kr}})\Delta_{kl}^{\text{Kr}} + (m_e/M_{\text{H}})\Delta_{kl}^{\text{H}}], \quad [3]$$

according to Watson's expression (*25*). In Eq. [3], μ_c is defined for KrH^+ as

TABLE 4
Observed Frequencies of Pure Rotational Transitions of $^{82}KrH^+$ (MHz)

$J' \leftarrow J''$	Observed frequency[a]	Obs. −Calc.[b]	Obs. −Calc.[c]
2 ← 1	989 043.997 (53)	−0.019	−0.028
3 ← 2	1 482 890.011 (52)	−0.008	−0.007
4 ← 3	1 975 925.274 (45)	0.016	0.032
5 ← 4	2 467 880.224 (36)	0.007	0.030
6 ← 5	2 958 485.999 (38)	−0.015	−0.006
7 ← 6	3 447 474.563 (46)	0.007	−0.034

[a] The numbers in parentheses are the estimated 1σ uncertainties in units of the last quoted digits.
[b] Calculated frequency from the rotational parameters in Table 5.
[c] Calculated frequency from the mass independent Dunham parameters in Table 6.

TABLE 5
Rotational Parameters of $^{82}KrD^+$, $^{84}KrD^+$, $^{86}KrD^+$, and $^{82}KrH^+$ (MHz)[a]

	$^{82}KrD^+$	$^{84}KrD^+$	$^{86}KrD^+$	$^{82}KrH^+$
B	125 849.9465(95)	125 778.4447(45)	125 710.2297(80)	247 351.1619(42)
D	2.89466(11)	2.891371(48)	2.888213(80)	11.27116(14)
H	$2.740(40)\times10^{-5}$	$2.735(14)\times10^{-5}$	$2.729(23)\times10^{-5}$	$2.198(15)\times10^{-4}$

[a] The numbers in parentheses are the estimated 1σ uncertainties in units of the last quoted digits.

$$\mu_c = M_{Kr}M_H/(M_{Kr} + M_H - m_e), \qquad [4]$$

where M_{Kr} and M_H are the atomic masses of krypton and hydrogen, respectively, and m_e the electron mass. We used the values of M_{Kr}, M_H, and m_e given in Ref. (*26*). In a previous analysis (*20*), the 11 parameters U_{10}, U_{20}, U_{01}, U_{11}, U_{21}, U_{02}, U_{12}, U_{03}, U_{04}, Δ_{01}^{Kr}, and Δ_{01}^{H} were included in Eq. [2], but only U_{01}, Δ_{01}^{Kr}, and Δ_{01}^{H} were fitted, setting other parameters to the values determined from the IR data (*6*). In our analysis, we at first fitted the parameters U_{02} and U_{03} as well as the parameters U_{01}, Δ_{01}^{Kr}, and Δ_{01}^{H}, fixing other parameters U_{10}, U_{20}, U_{11}, U_{21}, U_{12}, and U_{04} to the values determined from the IR data (*6*). Our data set consists of both the 61 FIR frequencies given in Tables 1–4, Ref. (*12*), and Ref. (*20*) and the 291 IR data reported in Ref. (*6*). These data were weighted inversely as the square of the experimental uncertainties. The uncertainties of all the IR data were assumed to be the same as 30 MHz, which is the value estimated for the stronger unblended lines (*6*). In this preliminary fit, we found a systematic deviation (~1 MHz) in the calculated frequencies of the rotational transitions. The inclusion of the higher-order parameter Δ_{02}^{H} reduces this deviation substantially. The determined parameters are shown in Table 6. In comparison with the previous values, the accuracy of the parameters U_{02} and U_{03} are improved, because the new accurate data on relatively high-J transitions contain the information on the centrifugal distortion. Our accurate data on the KrD^+ species allowed us to improve the accuracy of Δ_{01}^{H} and to determine the higher-order parameter Δ_{02}^{H} for the first time. However, the introduction of Δ_{02}^{H} causes a large difference in Δ_{01}^{Kr} from the previous value. This parameter Δ_{01}^{Kr} should be improved with the additional data on ^{78}Kr, ^{80}Kr, and ^{83}Kr isotopes.

We also observed several higher-J transitions ($J > 5$) of $^{83}KrD^+$ and $^{83}KrH^+$, but their hyperfine structures due to ^{83}Kr nuclear spin were not resolved. We failed to obtain their hypothetical transition frequencies, although the quadrupole coupling constant eqQ has already been determined (*12*). Hence, observed frequencies are not reported here. For these isotopic species we were not able to observe low-J transitions.

In summary, we observed the pure rotational spectra of $^{82}KrD^+$, $^{84}KrD^+$, $^{86}KrD^+$, and $^{82}KrH^+$ with an accuracy of a few hundred kilohertz. Effective rotational parameters B, D, and H of these ions were determined for the ground vibrational state. By analyzing the observed frequencies with the previous data, the mass independent Dunham parameters U_{02}, U_{03}, and Δ_{01}^{H} were determined more accurately and the higher-order parameter Δ_{02}^{H} was determined for the first time.

TABLE 6
Mass-independent Dunham Parameters of KrH^+ [a]

	This work	Previous work[b]
U_{01}	250 214.33(16)	250 214.66(15)
U_{02}	−11.22902(17)	−11.2358(17)[c]
U_{03}	$2.2340(27)\times10^{-4}$	$2.26(36)\times10^{-4}$ [c]
Δ_{01}^{Kr}	0.972(94)	0.682(70)
Δ_{01}^{H}	0.11533(18)	0.1172(20)
Δ_{02}^{H}	0.657(49)	—

[a] The unit of U_{kl} is MHz(amu)$^{(k/2+l)}$. Parameters Δ_{kl} are non-dimensional. The numbers in parentheses are the estimated 1σ uncertainties in units of the last quoted digits.
[b] Ref.(*20*).
[c] Fixed to the values reported in Ref.(*6*).

ACKNOWLEDGMENTS

The authors thank Mr. Ohtaki, Mr. Nagai, and Ms. Matsunaga for help in the experiment. This work was supported partly by a Grant-in-Aid from the Ministry of Education, Science and Culture of Japan (Grant 09490014).

REFERENCES

1. P. Bernath and T. Amano, *Phys. Rev. Lett.* **48,** 20–22 (1982).
2. M. W. Crofton, R. S. Altman, N. N. Haese, and T. Oka, *J. Chem. Phys.* **91,** 5882–5886 (1989).
3. Z. Liu and P. B. Davies, *J. Chem. Phys.* **107,** 337–341 (1997).
4. M. Wong, P. Bernath, and T. Amano, *J. Chem. Phys.* **77,** 693–696 (1982).
5. R. S. Ram, P. F. Bernath, and J. W. Brault, *J. Mol. Spectrosc.* **113,** 451–457 (1985).
6. J. W. C. Johns, *J. Mol. Spectrosc.* **106,** 124–133 (1984).
7. S. A. Rogers, C. R. Brazier, and P. F. Bernath, *J. Chem. Phys.* **87,** 159–162 (1987).
8. D. J. Liu, W. C. Ho, and T. Oka, *J. Chem. Phys.* **87,** 2442–2446 (1987).

9. W. C. Bowman, G. M. Plummer, E. Herbst, and F. C. De Lucia, *J. Chem. Phys.* **79,** 2093–2095 (1983).
10. K. B. Laughlin, G. A. Blake, R. C. Cohen, D. C. Hovde, and R. J. Saykally, *Phys. Rev. Lett.* **58,** 996–999 (1987).
11. K. B. Laughlin, G. A. Blake, R. C. Cohen, and R. J. Saykally, *J. Chem. Phys.* **90,** 1358–1361 (1989).
12. H. E. Warner, W. T. Conner, and R. C. Woods, *J. Chem. Phys.* **81,** 5413–5416 (1984).
13. H. Linnartz, M. Havenith, E. Zwart, W. L. Meerts, and J. J. ter Meulen, *J. Mol. Spectrosc.* **153,** 710–717 (1992); the data on $^{86}KrD^+$ are unpublished.
14. K. A. Peterson, R. H. Petrmichl, R. L. McClain, and R. C. Woods, *J. Chem. Phys.* **95,** 2352–2360 (1991).
15. K. M. Evenson, D. A. Jennings, and F. R. Petersen, *Appl. Phys. Lett.* **44,** 576–578 (1984).
16. I. G. Nolt, J. V. Radostitz, G. DiLonardo, K. M. Evenson, D. A. Jennings, K. R. Leopold, M. D. Vanek, L. R. Zink, A. Hinz, and K. V. Chance, *J. Mol. Spectrosc.* **125,** 274–287 (1987).
17. F. Matsushima, T. Oka, and K. Takagi, *Phys. Rev. Lett.* **78,** 1664–1666 (1997).
18. K. Takagi and F. Matsushima, abstracts K27, 15th Colloquium on High-Resolution Molecular Spectroscopy, Glasgow, 1997.
19. J. M. Brown, D. A. Jennings, M. Vanek, L. R. Zink, and K. M. Evenson, *J. Mol. Spectrosc.* **128,** 587–589 (1988).
20. H. Linnartz, L. R. Zink, and K. M. Evenson, *J. Mol. Spectrosc.* **184,** 56–59 (1997).
21. F. C. De Lucia, E. Herbst, G. M. Plummer, and G. A. Blake, *J. Chem. Phys.* **78,** 2312–2316 (1983).
22. F. Matsushima, H. Odashima, D. Wang, S. Tsunekawa, and K. Takagi, *Jpn. J. Appl. Phys.* **33,** 315–318 (1994).
23. K. V. Chance, T. D. Varberg, K. Park, and L. R. Zink, *J. Mol. Spectrosc.* **162,** 120–126 (1993).
24. J. L. Dunham, *Phys. Rev.* **41,** 721–731 (1932).
25. J. K. G. Watson, *J. Mol. Spectrosc.* **80,** 411–421 (1980).
26. I. Mills, T. Cvitaš, K. Homann, N. Kallay, and K. Kuchitsu, ''Quantities, Units, and Symbols in Physical Chemistry,'' Blackwell Scientific Publications Limited, Oxford, 1988.